

Measurements of Higgs boson properties in decays to two Tau leptons and search for lepton-flavor-violating Higgs boson decays into Tau leptons using the ATLAS detector

Ömer Oğul Öncel

Physikalisches Institut, Albert-Ludwigs-Universität Freiburg, D-79104 Freiburg, Germany

ogul.uncel@cern.ch



The 17th International Workshop on
Tau Lepton Physics (TAU2023)
Louisville, USA, 4-8 December 2023
doi:[10.21468/SciPostPhysProc.17](https://doi.org/10.21468/SciPostPhysProc.17)

Abstract

Three analyses exploiting the $H \rightarrow \tau\tau$ process using 139 fb^{-1} of proton–proton collision data collected at a center-of-mass energy of 13 TeV by the ATLAS detector at the LHC are presented. A measurement of VH production, with $V(= W, Z) \rightarrow e\nu/\mu\nu, ee/\mu\mu$ decays, has established the first evidence for this process with an observed (expected) significance of 4.2 (3.6) standard deviations. The second analysis, first of its kind by the ATLAS collaboration, probes CP-invariance if the decay products of the τ leptons using an angular observable ϕ_τ , and measured an observed (expected) value of $\phi_\tau = 9 \pm 16^\circ$ ($0 \pm 28^\circ$) at 68% confidence level. The last analysis is a search for lepton-flavour-violation in $H \rightarrow e\tau/\mu\tau$ decays, where most stringent exclusion limits at 95% confidence level on $H \rightarrow e\tau$ branching ratio of 0.2%, is obtained.



Copyright Ö. O. Öncel.

This work is licensed under the Creative Commons
[Attribution 4.0 International License](https://creativecommons.org/licenses/by/4.0/).

Published by the SciPost Foundation.

Received 2024-04-29

Accepted 2024-12-19

Published 2025-07-23

doi:[10.21468/SciPostPhysProc.17.013](https://doi.org/10.21468/SciPostPhysProc.17.013)



Check for
updates

1 Introduction

The Standard Model (SM) Higgs boson production at the LHC originating from proton–proton collisions at a center-of-mass energy of 13 TeV is dominated by four processes: gluon-gluon fusion (87%), vector-boson fusion (7%), Higgs-strahlung (4%) and heavy-flavour associated production (2%). Higgs boson decays into a pair of τ leptons has been observed in 2018 [1] and has a branching fraction of 6%. Three analyses using this decay channel are summarized: cross-section measurement of the VH process [2], measurement of charge conjugation and parity (CP) properties in τ lepton decay planes [3], and a search for lepton-flavour-violation (LFV) [4].

All three analyses are conducted using 139 fb^{-1} of data collected by the ATLAS [5] detector and share common objects and event reconstruction techniques. Leptonically decaying τ leptons are reconstructed as the light lepton ($\ell = e, \mu$) they decay into. Hadronically decaying τ leptons are reconstructed using a Recurrent Neural Network [6] that processes visible decay products. The invariant mass of the di- τ -lepton system is estimated using the likelihood-based Missing Mass Calculator [7], except in the WH channel of the VH analysis where transverse-projection two-parent mass variable M_{2T} [8] is used.

2 Evidence for VH , $H \rightarrow \tau\tau$ process

The measurement is performed by selecting the semileptonic ($\tau_{\text{lep}}\tau_{\text{had}}$) and hadronic ($\tau_{\text{had}}\tau_{\text{had}}$) Higgs boson and $V(=W, Z) \rightarrow e\nu/\mu\nu, ee/\mu\mu$ decays. WH and ZH channels are distinguished and separately optimized. The important challenges in this analysis are the ambiguities in correctly selecting and assigning intermediate parent particles due to multiple sources of ℓ/ν .

Background processes are estimated from simulated event samples except the processes in which a jet is misidentified as a light lepton or hadronically decaying τ lepton. These contributions are estimated using the data-driven Fake-Factor method [2].

Neural networks (NNs) are used to separate signal from the dominant diboson ($VV = WZ, ZZ$) background processes. One NN is trained in each channel, except in the $WH(\tau_{\text{lep}}\tau_{\text{had}})$ process, which has individual NN discriminants for each of the final states containing $ee, e\mu$ and $\mu\mu$ decays. NN distribution in the $ZH(\tau_{\text{lep}}\tau_{\text{had}})$ region is shown in Fig. 1 on the left. Input variables encoding both kinematic properties of the particles (e.g. p_T, η, ϕ) and total event level information (e.g. missing transverse energy) are used in the training.

2.1 Results

NN distributions in four signal regions (SRs) are used in a binned profile-likelihood fit to extract the signal strength μ , which is the ratio of the measured cross-section to the SM prediction. Combined post-fit distribution from all SRs are shown in Fig. 1 on the right. The measurement is dominated by the statistical uncertainties. The leading source of systematic uncertainty is from the reconstruction of hadronic τ lepton decays. The signal strength is found to be $\mu = 1.28^{+0.30}_{-0.29} \text{ (stat.)}^{+0.25}_{-0.21} \text{ (syst.)}$. The observed (expected) statistical significance of the measurement is 4.2 (3.6) standard deviations. This result provides the first evidence for this process.

3 Measurement of the CP properties in $H \rightarrow \tau\tau$ decay products

This analysis aims at measuring the CP properties of the interaction between the Higgs boson and τ leptons by studying the relation between the amount of CP-mixing and the transverse-spin correlations of the τ leptons. The effect is carried over to the τ -decay products and quantified by the observable ϕ_{CP}^* , the signed acoplanarity angle between the decay planes of the τ leptons [9]. CP-mixing manifests itself as a phase-shift in ϕ_{CP}^* .

Misidentified jets are estimated using the Fake-Factor method similar to the VH analysis [2]. All other background processes are estimated from simulated event samples.

Inclusive SRs are defined with low- and high-purity Boost/VBF topology selections, which are separately constructed for $\tau_{\text{lep}}\tau_{\text{had}}$ and $\tau_{\text{had}}\tau_{\text{had}}$ final states. Eight $Z \rightarrow \tau\tau$ control regions (CRs) are defined, each corresponding to one of the inclusive SRs. Furthermore, two different CRs are defined to constrain the energy resolution for the reconstruction of π^0 mesons.

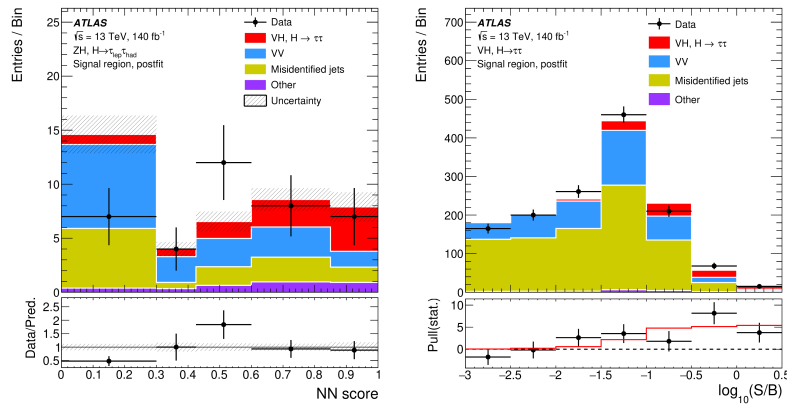


Figure 1: Post-fit distribution of the NN score in $ZH(\tau_{\text{lep}}\tau_{\text{had}})$ region (left); Post-fit distribution of the logarithm of signal-to-background ratio of combined yields of all SRs (right). Shaded bands represent both, statistical and systematic uncertainties [2].

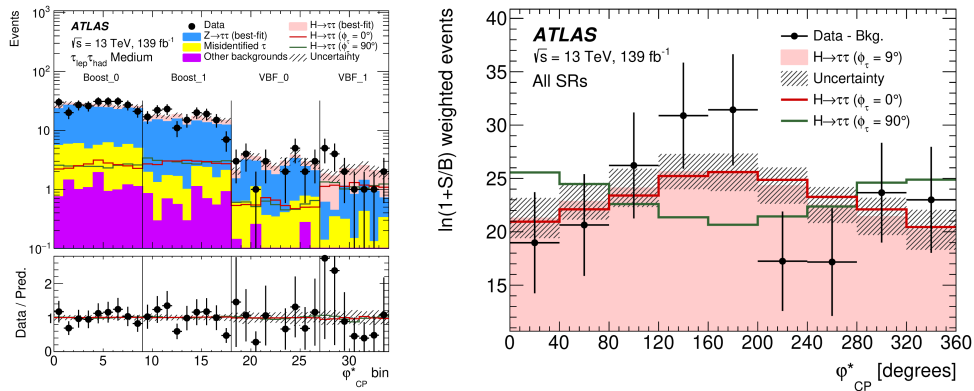


Figure 2: Post-fit distribution of ϕ_{CP}^* in the *medium* SRs (left); Best-fit yields of all SRs combined, weighted by $\ln(1+S/B)$ where S (B) stands for Signal (Background). Green (red) overlaid lines represent the pure CP-even (CP-odd) signal hypotheses, scaled to the best-fit signal yield (right). Shaded bands represent both, statistical and systematic uncertainties [3].

Each of the eight inclusive SRs are further split into three (low, medium and high) subregions of increasingly optimized ϕ_{CP}^* sensitivity, according to the different decay-plane reconstruction methods used. The SRs for the *medium* subregion are shown in Fig. 2 on the left.

3.1 Results

A binned profile-likelihood fit is performed simultaneously in all SRs and CRs. The normalization of Higgs boson production is left unconstrained in order to probe only the shape information. The combined yields in all SRs, with different CP-mixing hypotheses is shown in Fig. 2 on the right. The observed (expected) value of the angular observable is $\phi_\tau = 9 \pm 16^\circ$ ($0 \pm 28^\circ$). The results are in agreement with the SM prediction within 1 standard deviations (σ), whereas the pure CP-odd hypothesis is rejected with 3.4σ . The analysis is statistically limited. Among the systematic uncertainties, jet energy scale/resolution has the highest impact.

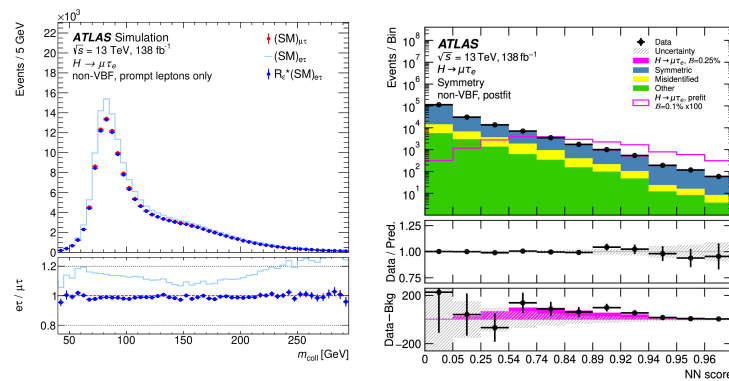


Figure 3: Collinear mass distribution in the non-VBF region comparing SM $e\tau$ events represented by a cyan line, to efficiency-corrected SM $e\tau$ events shown as blue dots. SM $\mu\tau$ events are depicted as red dots. Only statistical uncertainties are shown (left); Post-fit NN score distribution in $H \rightarrow e\tau$, non-VBF SR using the Symmetry method. Pre-fit signal hypothesis assuming a branching ratio of 0.1% is overlayed as a violet coloured line and scaled by a factor of 100 for visibility. Shaded bands represent both, statistical and systematic uncertainties (right) [4].

4 Search for LFV decays in $H \rightarrow e\tau/\mu\tau$ processes

Searches for LFV in the $H \rightarrow e\tau$ and $H \rightarrow \mu\tau$ decays are performed by splitting the ℓ , τ_{lep} and ℓ , τ_{had} final states into VBF (more than two jets) and non-VBF regions [4].

Misidentified objects are estimated using the Fake-Factor or ABCD methods. For the rest, two background estimation methods are used: in the first case a data-assisted MC-template method is used to estimate $Z \rightarrow \tau\tau$ and background from Top-quark production. In the second case backgrounds with prompt leptons are estimated by the Symmetry method [10], which relies on the $e \leftrightarrow \mu$ symmetry present in the SM, once the processes are efficiency-corrected for the asymmetries originating from instrumental effects (see Fig. 3, left).

Binary (multi) classifier discriminants are trained for non-VBF (VBF) event topologies to separate signal from various type of backgrounds, employing Boosted Decision Trees (NNs) when using the MC-template (Symmetry) method. An example NN score distribution is shown in Fig. 3 on the right.

4.1 Results

Various binned profile-likelihood fits, combining the background estimation methods mentioned, are performed on all SRs and CRs. The observed (expected) upper limits for branching ratios of $H \rightarrow e\tau$ and $H \rightarrow \mu\tau$ at 95% confidence level are 0.20% (0.11%) and 0.18% (0.09%), respectively. Results estimated using different background estimation methods are compatible with each other. The analysis is systematically limited, where background sample size and the misidentified background uncertainties are found to be dominant.

5 Conclusion

Three analyses exploiting the $H \rightarrow \tau\tau$ decay channel, using 139 fb^{-1} proton-proton collision data collected by the ATLAS detector at the LHC at a center-of-mass energy of 13 TeV are presented. The VH analysis provided the first evidence for this process. A first search for CP-violation search by ATLAS collaboration in this decay channel using an angular observable

formed by the τ lepton decay products, yielded results in agreement with SM within 1σ . The search for LFV resulted in the most stringent exclusion limit of 0.2% at 95% confidence level to date on the $H \rightarrow e\tau$ branching ratio.

Acknowledgments

Funding information The author is funded by the Federal Ministry of Education and Research (BMBF) within the project 05H21VFCA3 “(ErUM-FSP T02) - Run 3 von ATLAS am LHC: Untersuchung des elektroschwachen Sektors mit dem ATLAS-Experiment am Large Hadron Collider”.

References

- [1] M. Aaboud et al., *Cross-section measurements of the Higgs boson decaying into a pair of τ -leptons in proton-proton collisions at $\sqrt{s} = 13$ TeV with the ATLAS detector*, Phys. Rev. D **99**, 072001 (2019), doi:[10.1103/PhysRevD.99.072001](https://doi.org/10.1103/PhysRevD.99.072001).
- [2] G. Aad et al., *Measurement of the $VH, H \rightarrow \tau\tau$ process with the ATLAS detector at 13 TeV*, Phys. Lett. B **855**, 138817 (2024), doi:[10.1016/j.physletb.2024.138817](https://doi.org/10.1016/j.physletb.2024.138817).
- [3] G. Aad et al., *Measurement of the CP properties of Higgs boson interactions with τ -leptons with the ATLAS detector*, Eur. Phys. J. C **83**, 563 (2023), doi:[10.1140/epjc/s10052-023-11583-y](https://doi.org/10.1140/epjc/s10052-023-11583-y).
- [4] G. Aad et al., *Searches for lepton-flavour-violating decays of the Higgs boson into $e\tau$ and $\mu\tau$ in $\sqrt{s} = 13$ TeV pp collisions with the ATLAS detector*, J. High Energy Phys. **07**, 166 (2023), doi:[10.1007/JHEP07\(2023\)166](https://doi.org/10.1007/JHEP07(2023)166).
- [5] G Aad et al., *The ATLAS experiment at the CERN Large Hadron Collider*, J. Instrum. **3**, S08003 (2008), doi:[10.1088/1748-0221/3/08/S08003](https://doi.org/10.1088/1748-0221/3/08/S08003).
- [6] ATLAS collaboration, *Identification of hadronic tau lepton decays using neural networks in the ATLAS experiment*, Tech. Rep. ATL-PHYS-PUB-2019-033, CERN, Geneva, Switzerland (2019), <http://cds.cern.ch/record/2688062>.
- [7] G. Aad et al., *Measurements of Higgs boson production cross-sections in the $H \rightarrow \tau^+\tau^-$ decay channel in pp collisions at $\sqrt{s} = 13 = 13$ TeV with the ATLAS detector*, J. High Energy Phys. **08**, 175 (2022), doi:[10.1007/JHEP08\(2022\)175](https://doi.org/10.1007/JHEP08(2022)175).
- [8] A. J. Barr, T. J. Khoo, P. Konar, K. Kong, C. G. Lester, K. T. Matchev and M. Park, *Guide to transverse projections and mass-constraining variables*, Phys. Rev. D **84**, 095031 (2011), doi:[10.1103/PhysRevD.84.095031](https://doi.org/10.1103/PhysRevD.84.095031).
- [9] S. Berge, W. Bernreuther, B. Niepelt and H. Spiesberger, *How to pin down the CP quantum numbers of a Higgs boson in its τ decays at the LHC*, Phys. Rev. D **84**, 116003 (2011), doi:[10.1103/PhysRevD.84.116003](https://doi.org/10.1103/PhysRevD.84.116003).
- [10] S. Bressler, A. Dery and A. Efrati, *Asymmetric lepton-flavor violating Higgs boson decays*, Phys. Rev. D **90**, 015025 (2014), doi:[10.1103/PhysRevD.90.015025](https://doi.org/10.1103/PhysRevD.90.015025).